Incorporation of artificial neural networks and data assimilation techniques into a third-generation wind–wave model for wave forecasting

Zhixu Zhang, Chi-Wai Li, Yiquan Qi and Yok-Sheung Li

ABSTRACT

Although the third-generation formulation of the ocean wave model describes the wave generation, dissipation and nonlinear interaction processes explicitly, many empirical parameters exist in the model which have to be determined experimentally. With the advance in oceanographic remote-sensing techniques, information on oceanic parameters including significant wave height (SWH) can be obtained daily by satellite altimeters. The assimilation of these data into the wave model provides a way of improving the hindcasting results. However, for wave forecasting, no altimeter data exist during the forecasting period, by definition. To improve the forecasting accuracy of the wave model, Artificial Neural Networks (ANN) are introduced to mimic the errors introduced by the wave model. This is achieved by training the ANN using the wave model output as input, and the results after data assimilation as the targeted output. The trained ANN is then used as a post-processor of the output from the wave model. The proposed method has been applied in wave simulation in the northwestern Pacific Ocean. The statistical interpolation method is used to assimilate the altimeter data into the wave model output and a back-propagation ANN is used to mimic the relation between the wave model outputs with or without data assimilation. The results show that an apparent improvement in the accuracy of forecasting can be obtained.

Key words | artificial neural networks, data assimilation, wave forecast, wind–wave model

Zhixu Zhang
Department of Civil and Structural Engineering,
The Hong Kong Polytechnic University,
Hong Kong,
PR China, and South China Sea Institute of Oceanology,
Chinese Academy of Sciences,
Guangzhou,
PR China

Chi-Wai Li (corresponding author)
Yok-Sheung Li
Department of Civil and Structural Engineering,
The Hong Kong Polytechnic University,
Hong Kong,
PR China
Fax: +852 2334 6389;
E-mail: *cecwli@polyu.edu.hk*

Yiquan Qi
South China Sea Institute of Oceanology,
Chinese Academy of Sciences,
Guangzhou,
PR China

INTRODUCTION

The third-generation ocean wave model is widely used currently to hindcast and forecast wind generated waves. Examples of this type of model include WAM (WAMDI Group 1988), SWAN (Booij *et al.* 1999) and WAVEWATCH (Tolman 1999), as well as Li (1992). In these models all the wave generation, dissipation and nonlinear interaction processes are described explicitly. However, due to our limitation in the understanding of the physics of the processes and the difficulties in expressing the processes in a simple way, many empirical parameters are introduced into the model which need to be determined experimentally. The results computed by these models are, on the whole, satisfactory, but they are sensitive to some of the model parameters, particularly the wind input.

Further improvement of the modeling results is possible if measured data are available. With the advance in oceanographic remote-sensing techniques, information on oceanic states including significant wave height (SWH) can be obtained daily by satellite altimeters. The assimilation of these data into the output of the wave model provides a way of improving the hindcasting results.

A great deal of work has been done on data assimilation into numerical models. They can be classified into four categories as follows (Refsgard 1997):

doi: 10.2166/jh.2006.005

(a) updating of input parameters,
(b) updating of state variables (e.g. Kalman filtering),
(c) updating of model parameters,
(d) updating of output variables.

The main difference between method (b) and method (d) is that in method (b) the data assimilation process is integrated into the model and the solution procedure has to be modified, while in method (d) the data assimilation procedure and the solution procedure for the model are detached. In the assimilation of wave data into numerical models, method (d) is commonly employed, mainly because it is easily implemented. Komen (1985) applied a simple updating technique to assimilate the wave buoy data into a coupled hybrid wave model GONO (Janssen *et al.* 1984) in the prediction of swell propagation. Thomas (1988) developed a scheme to update the wave spectrum using the buoy data of SWH and wind speed. Following the JONSWAP spectral shape, the wave age is maintained by rescaling the energy and peak frequency of the wind–sea part of the spectrum using the wind speed. The swell part of the spectrum is scaled according to the energy only. Esteva (1988) proposed a scheme to adjust the wave spectrum by a constant scaling using the SEASAT SWH data. Bauer *et al.* (1992) performed a global assimilation of SEASAT SWH data into the WAM model. Similar to Esteva (1988), a constant scaling is used for the adjustment. The difference is that the adjustment was carried out over a larger area, instead of just at the observation point. All these schemes produce an improvement in the model prediction results to certain extents.

Lionello *et al.* (1992) used the technique of optimal interpolation to assimilate the SEASAT and GEOSAT SWH data into the WAM model. The wave spectrum is partitioned into wind–sea and swell. The wind–sea part of the spectrum is updated using JONSWAP relationships, which is similar to Thomas (1988). The difference with the above schemes is that the swell part of the spectrum is updated with the amplitude and frequency changes such that the swell steepness is maintained. The advantages of this approach are that the dissipation and energy transfer within the swell spectrum are unchanged and the correction decay times are increased significantly.

Although data assimilation is effective to improve the model prediction results, it may not be effective in forecasting because during the forecasting period there will be no data available. The information of the data retained in the model will decay with time and the model results will be identical to those without data assimilation after a sufficiently long period of time. Under this situation it is highly desirable if the effect of data assimilation can be mimicked and introduced into the model during the forecasting period. An artificial neural network (ANN) is a kind of method which can be used for this purpose.

ANN is a kind of computing system that mimics a simplified model of the human brain by organizing neurons into a network. It is trained to give acceptable results based on past information. This method is very flexible and has been applied in a wide range of engineering problems, particularly in complex nonlinear dynamical systems. In the areas of ocean engineering and oceanography, Li (2000) and Tsai *et al.* (2002) applied ANN to correlate SWH at neighbouring stations. Deo & Kumar (2000) used ANN to interpolate wave heights at unknown points.

In the present work, ANN will be used to mimic the effect of data assimilation into a third-generation wave model. For the data assimilation component, the TOPEX/Poseidon altimeter SWH data will be used and the statistical interpolation method will be employed. The model will be applied to forecast wind waves generated in the northwestern Pacific Ocean region. The performance of the model will then be evaluated.

WAVE MODEL

In the third-generation wave model the equation used for wave predictions represents the energy conservation of a wave component of frequency f and direction θ measured from a reference axis (e.g. WAMDI Group 1988; Li 1992):

$$\frac{\partial F}{\partial t}+\frac{\partial}{\partial x}(c_g\cos\theta F)+\frac{\partial}{\partial y}(c_g\sin\theta F)+\frac{\partial}{\partial\theta}\left[\frac{c_g}{c}\left(\sin\theta\frac{\partial c}{\partial x}-\cos\theta\frac{\partial c}{\partial y}\right)F\right]=S_{in}+S_{nl}+S_{ds}+S_{bf} \quad (1)$$

$$c_g=0.5\left[\frac{g}{k}\tanh(kd)\right]^{1/2}\left[1+\frac{2kd}{\sinh(2kd)}\right]$$

$$\sigma=2\pi f=[gk\tanh(kd)]^{1/2}\ \text{ and }\ c=[g/k\tanh(kd)]^{1/2}$$

where $F(f, \theta, x, y, t)$ is the spectral density, c_g is the group velocity, σ is the angular frequency, c is the phase velocity and d is the water depth. The source functions take account of several energy input and dissipation processes: wind input S_{in}, nonlinear transfer S_{nl}, white-capping dissipation S_{ds} and bottom friction S_{bf}.

Different numerical schemes have been adopted to solve the governing equation by different models. In this work, the numerical model of Li (1992) is employed which utilized a split operator scheme to solve the governing equation. The advection terms are solved by the bilinear-characteristics method, while the source and sink terms are solved by a quasi-second-order explicit scheme.

The model has been extensively applied in the coastal areas of Hong Kong and in the South China Sea region. It has been found that the model in general under-predicts the wave heights during the typhoon period. Similar results have been reported by using WAM in the Australian region (Bender & Glowacki 1996) and in the SEASAT studies (Bauer *et al.* 1996). Reasons for the inaccuracy in the prediction may be due to the inaccurate physics included in the model and/or under-prediction of surface wind speeds.

ASSIMILATION METHOD – STATISTICAL INTERPOLATION

The univariate two-dimensional Statistical Interpolation (SI) method (Gandin 1963) is commonly used in assimilating data into wave models. In this method, the analysed SWH at every grid point i, H_a^i, is expressed as a linear combination of the predicted value from the model, H_p^i, and the observed values at or close to point i, H_o^i:

$$H_a^i = H_p^i + \sigma_p^j \sum_{j=1}^{N} W_{ij} \left[\frac{H_o^j - H_p^j}{\sigma_p^j} \right] \tag{2}$$

where σ_p is the model prediction root mean squares (RMS) error and W_{ij} is the weight chosen to minimize the RMS error of the analysis. By assuming that the errors in the model are uncorrelated with the errors in the measurement, the weight is given by

$$W_{ij} = \sum_{k=1}^{N} P_{ik} M_{kj}^{-1} = \sum_{k=1}^{N} P_{ik} (P + O)_{kj}^{-1} \tag{3}$$

where P is the error correlation matrix of the model prediction and O is the error correlation matrix of the observations.

The observation errors are assumed uncorrelated and are usually set to a constant value ϵ:

$$O_{kj} = \varepsilon \tag{4}$$

The prediction error correlation matrix is difficult to specify. It is plausible that the correlation scales will vary spatially and temporally. The commonly used approach is to assume the matrix has an isotropic exponential form (e.g. Lionello *et al.* 1992; Bender & Glowacki 1996; Greenslade 2001):

$$P_{kj} = \mathbf{exp}\left(\frac{-|x_k - x_j|}{L} \right) \tag{5}$$

where L is the correlation length scale and $|x_k - x_j|$ is the distance between points k and j.

Adjustment of wave spectra

The output of the wave model at each grid point is the two-dimensional (2D) wave spectrum, while the data used in assimilation is SWH which is proportional to the square root of the total wave energy. There is no unique way to adjust the wave spectrum based on SWH. The approach used in the present study follows that of Greenslade (2001). First the wave spectrum is divided into wind–sea wave components and swell wave components. Wind–sea is the wave component propagating in direction θ with phase speed c_p, which satisfies the following condition:

$$\frac{28|u_*|}{c_p} \cos(\theta - \theta_w) > 1 \tag{6}$$

where u_* is the friction velocity and θ_w is the wind direction. The rest are the swell wave components. For wind–sea, a simple scaling is used to adjust the wave components. The formula is given by

$$F_a^i(f, \theta) = a^i F_p^i(f, \theta) \tag{7}$$

where F_a^i is the analyzed spectrum at grid-point i, F_p^i is the predicted spectrum, f is the frequency, θ is the direction and

$$a^i = \left(\frac{H_a^i}{H_p^i} \right)^2. \tag{8}$$

The slope of the spectrum and thus the dissipation term will be altered by such scaling. For swell, the spectral slope is kept constant and the energy is scaled as follows:

$$F_a^i(f,\theta) = a^i F_p^i(f + \Delta f, \theta) \tag{9}$$

where

$$\Delta f = f_p - \left(\frac{f_p}{(a^i)^{1/4}}\right) \tag{10}$$

ARTIFICIAL NEURAL NETWORKS (ANN)

A multi-layered ANN is used and shown in Figure 1. It consists of one input layer, one or more hidden layers and one output layer. A number of nodes (neurons) are employed by each layer and each node is connected to the nodes in the adjacent layers with different weights. The node possesses a threshold value for controlling the output. Each node receives signals from those nodes in the adjacent layer closer to the input layer linearly weighted by the interconnected weighting values between the nodes. The node then produces an output signal by sending the summed signal minus the threshold value through a transfer function. According to the deviation of the output value from the target value (the measured datum), weights and threshold values of the network are adjusted to reduce the output error. This can be done in many ways and the one that is used is called the backpropagation algorithm.

Consider Figure 1, an ANN with 1 hidden layer, where the input to the network is x_i, $i = 1, \ldots, N_{inp}$, where x_i are the nodal values (wave heights in the present study) and N_{inp} is the number of nodes in the input layer. Outputs of the hidden layer of nodes are

$$y_j = g\left(a_{0j} + \sum_{i=1}^{N_{inp}} a_{ij} x_i\right), \quad j = 1, \ldots, N_{hid} \tag{11}$$

where y_j are the nodal values and N_{hid} is the number of nodes in the hidden layer. Outputs of the output layer are

$$zk = g\left(b_{ok} + \sum_{j=1}^{N_{hid}} b_{jk} y_j\right), \quad k = 1, \ldots, N_{out} \tag{12}$$

where z_k are the nodal values and N_{out} is the number of nodes in the output layer. The transfer function g can have several forms; they can be asymmetric sigmoid functions, symmetric hyperbolic tangent functions or linear functions.

In total, there are $(N_{inp} + 1)N_{hid} + (N_{hid} + 1)N_{out}$ parameters (weights a and b) to be determined. This is achieved by training the ANN such that the mean squared error in reproducing reality (observed wave data) is minimal. The mean squared error is usually expressed as

$$E = \frac{1}{N_s}\sum_{1}^{N_s} (D_i - C_i)^2 \tag{13}$$

where N_s is the number of samples used, D is the desired output (measured value) and C is the computed output from the ANN. Since the functional form of E is known, it is possible to use gradient-based methods to find the minimum value of E and hence determine the values of parameters a and b. After training, the network can be applied to hindcast the desired variable. In the present study, the input data are the computed SWH without the data assimilation effect and the output are the SWH with the simulated data assimilation effect.

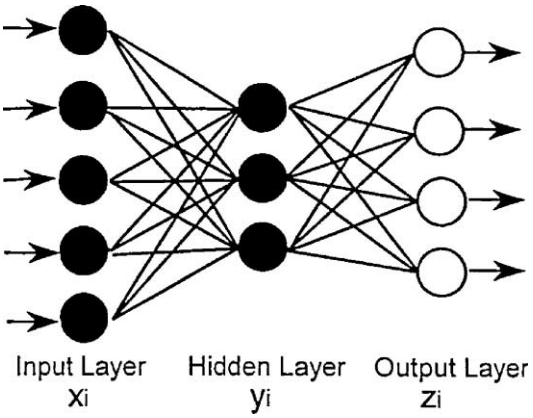

Figure 1 | The structure of a backpropagation ANN with one hidden layer.

ASSIMILATING SWH DATA INTO THE WAVE MODEL

The performance of the assimilation of altimeter data into the wave model is first investigated. The northwestern Pacific Ocean is chosen as the test region. The computational region covers 99°E – 170°E and 2°S – 50°N (Figure 2). The period of simulation is from 1 June to 31 August 2001. The computational time step is 30 min. The wind field is given by NOAA and is reanalyzed. It is of 3 h interval and

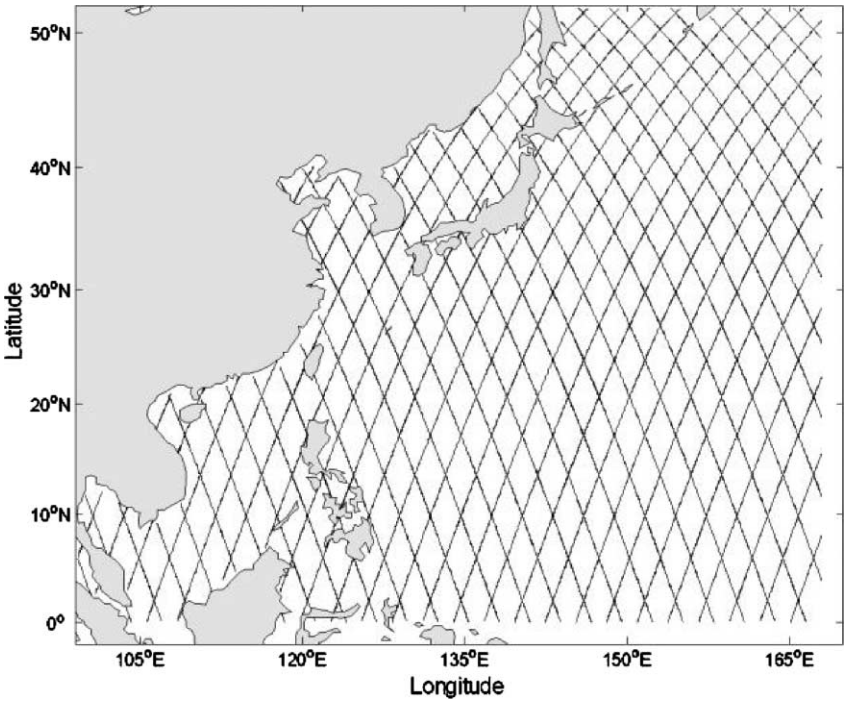

Figure 2 | The computational domain with the loci of the satellite altimeter.

$1° \times 1°$ resolution. Interpolation is thus required to obtain the input wind field of 30 min interval. The wave spectrum is divided into 25 frequency bands in logarithmic scale, ranging from 0.05 to 0.4 Hz, and 12 directional bands with 30° resolution. The use of such inequal frequency bands results in a higher resolution at the low frequency region, and more efficient computation of the nonlinear energy transfer among frequency bands.

The initial condition chosen in the model is a JONSWAP spectrum with a peak frequency of 0.3 Hz. A non-zero initial condition is essential in the model to trigger the growth of the waves. At outflow boundaries (water–water or land–water boundaries), the use of the characteristics-based scheme for the advection terms in the model automatically imposes a radiation boundary condition to allow outgoing waves leaving the computational domain with little disturbance. At inflow boundaries, the boundary condition will depend on the wave condition outside the computational domain. At a water–land boundary, a zero spectral value is imposed. At a water–water boundary, a zero gradient is imposed.

The correlation length scale L in Equation (5) should be determined first before the data assimilation procedure can be implemented. This is an empirical parameter and different values have been used by different investigators. Lionello *et al.* (1992) set L equal to 1650 km, Francis & Stratton (1990) set L equal to 1200 km, while Young & Glowacki (1996) set L equal to 350 km. In the present study, the value of L is chosen as 700 km, taking into consideration the space and time intervals of the loci of the satellite.

The loci of the satellite passing over the test region are shown in Figure 2. The time interval between one ascending path and the subsequent descending path is approximately 2 h. The computed field of SWH at the instant corresponding to period 321, locus 177 of the altimeter (1:00, 8 June 2001) is shown in Figure 3. By assimilating the altimeter data using the statistical interpolation method, the SWH field is changed and shown in Figure 4. It is clear the assimilated data exert an apparent effect on the spatial structure of the SWH field. The improvement in the prediction is shown in Figure 5 which displays the variation of SWH along a Lagrangian path traced by the satellite. It seems that the wave model consistently under-predicts the wave height. One possible explanation is that the values of the parameters calibrated in the wave model are not applicable in this region and error occurs. Further results

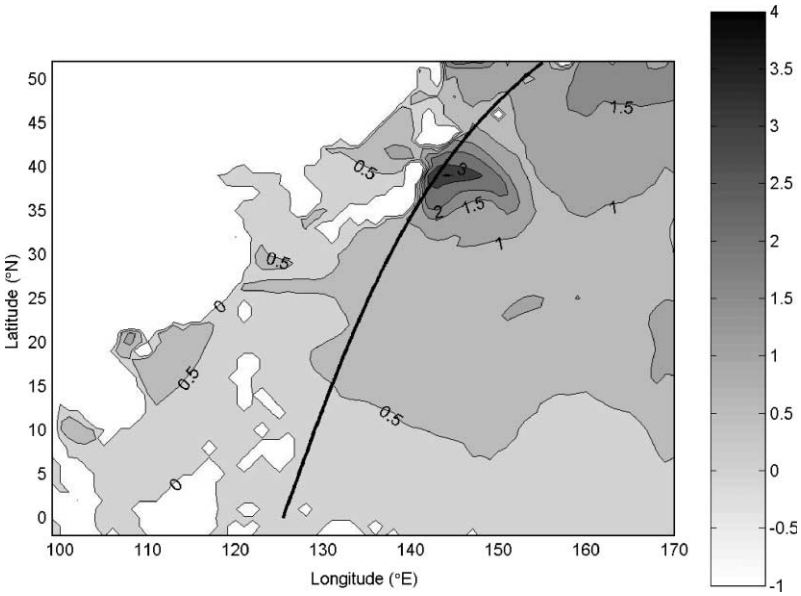

Figure 3 | Contours of SWH computed by wave model without data assimilation at 1 am, 8 June 2001.

at a different time period (7:00, 2 July 2001) are shown in Figure 6 and the same conclusion can be drawn.

The above results clearly show that data assimilation is successful in improving the wave model results. However, for wave forecasting, data will not be available by definition. When the data assimilation process is stopped, the computed waves will gradually return to the original computed values without the implementation of the data assimilation technique. Figure 7 displays the time history of the SWH at 133°E and 23°N. The result for the case with data assimilation is

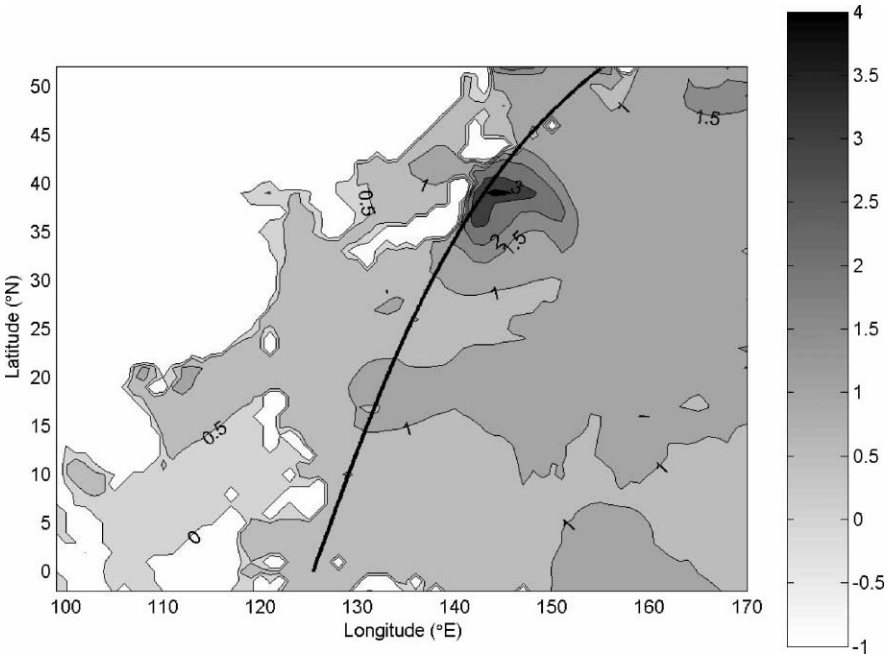

Figure 4 | Contours of SWH computed by wave model with data assimilation at 1 am, 8 June 2001.

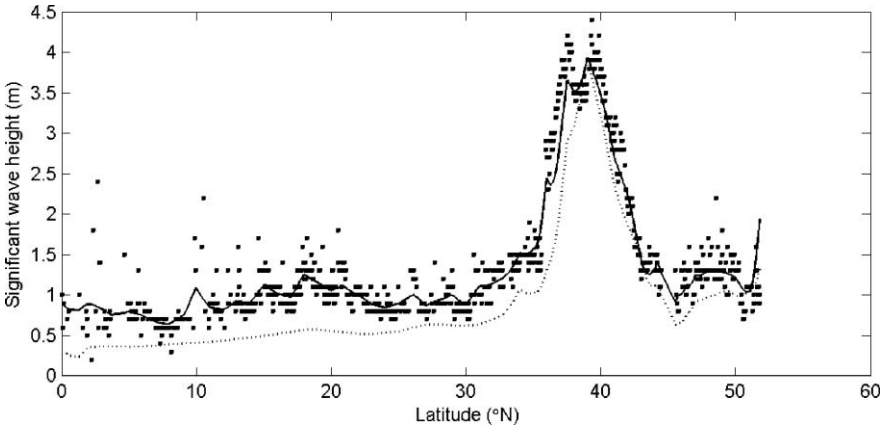

Figure 5 | SWH along the locus of the altimeter at 8 June 2001 (solid line – with data assimilation, dotted line – without data assimilation, symbol – observed values).

represented by the semi-dotted line and the result for the case without data assimilation is represented by dotted line. When the data assimilation procedure is stopped at hour 1097, the computed value immediately deviates from the result for the case with data assimilation. It becomes very close to the result for the case without data assimilation after hour 1250. Thus the effect of data assimilation will disappear in around 50 h for this example.

USING ANN TO MIMIC THE EFFECT OF DATA ASSIMILATION

The effect of data assimilation on the wave model output seems to be deterministic. This is due to the fact that the wave model always under-predicts the SWH recorded by the altimeter. In the absence of SWH data, the data assimilation effect can be predicted if it is stationary. ANN will be an effective tool to predict this effect. It can be trained with the computed SWH from the wind model as input and the computed SWH from the wind model with data assimilation as the target output.

In the above computational region, four output points have been chosen. The period of simulation is still from 1 June to 31 August 2001. The first 30 h is the start-up period of the model. ANN training is performed for the next 1000 h (1000 data) and ANN verification is carried out for the next 800 h (800 data). The results of ANN training at point A are shown in Figure 8. The RMS difference between

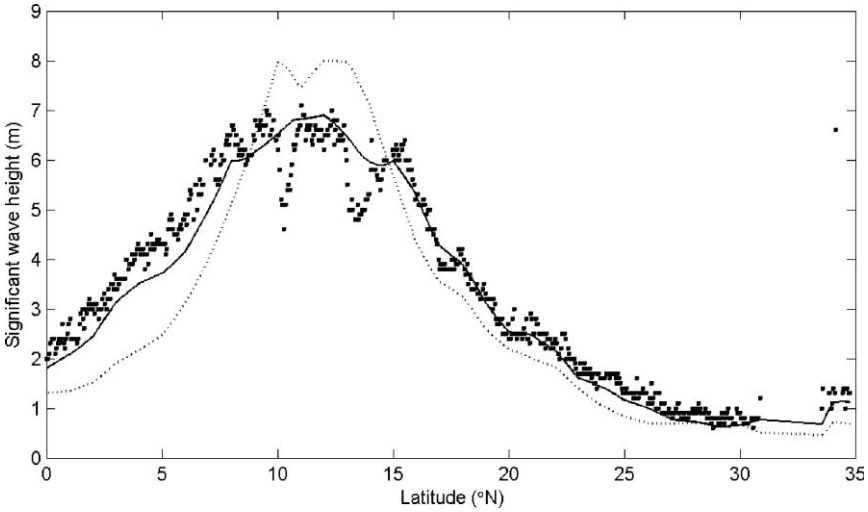

Figure 6 | SWH along the locus of the altimeter at 29 August 2000 (solid line – with data assimilation, dotted line – without data assimilation, symbol – observed values).

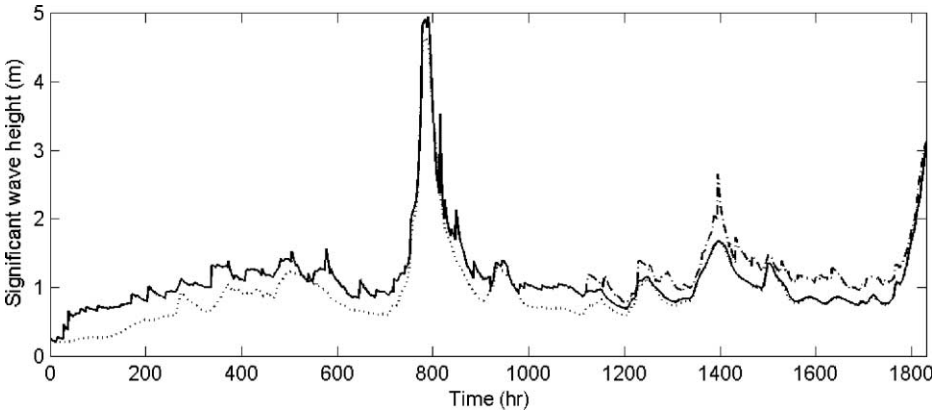

Figure 7 | Effect of stopping the data assimilation process (dotted line – without data assimilation, solid line – data assimilation process stopped at 1097 h, semi-solid line – with data assimilation).

the results with or without data assimilation is 0.284 m, while the RMS difference between the results after ANN training and the results with data assimilation is 0.097 m. At the verification stage, the RMS difference between the results with or without data assimilation is 0.287 m, while the RMS difference between the results after ANN training and the results with data assimilation is 0.073 m. The results clearly demonstrate that ANN is effective in reproducing the effect of data assimilation.

Table 1 displays the performances of ANN for the four different points. The difference in RMS values between the ANN output and the results with data assimilation at each point are substantially smaller than those between the results with or without data assimilation. The results for the training and verification of ANN at points B, C and D are shown in Figures 9–16. They show that ANN consistently improve the wave forecasting accuracy by introducing an effect similar to that of data assimilation.

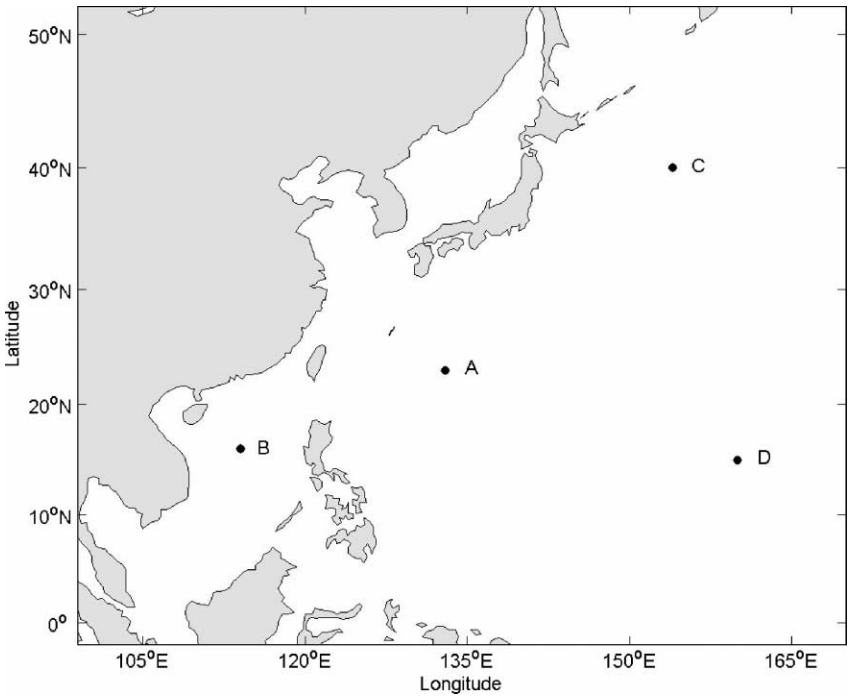

Figure 8 | Four output points for ANN training and verification (A: 133°E, 23°N; B: 114°E, 16°N; C: 154°E, 40°N; D: 160°E, 15°N).

Table 1 | Differences in RMS values between the results with and without data assimilation, and those between the results with ANN and without ANN

	Point A		Point B		Point C		Point D	
	Training	Hindcast	Training	Hindcast	Training	Hindcast	Training	Hindcast
RMS (with data assimilation-without data assimilation)	0.284 m	0.287 m	0.164 m	0.173 m	0.146 m	0.128 m	0.317 m	0.302 m
RMS (with ANN-without ANN)	0.097 m	0.073 m	0.079 m	0.079 m	0.101 m	0.097 m	0.093 m	0.077 m

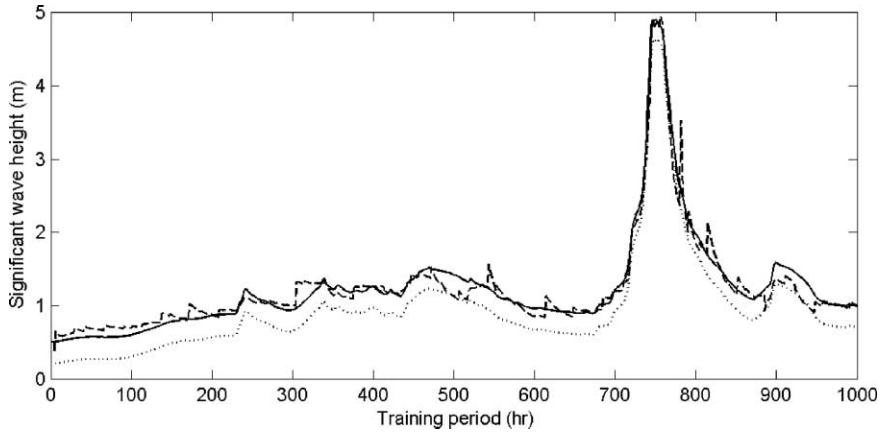

Figure 9 | Training of ANN at point A (dashed line – with data assimilation, solid line – ANN training results, dotted line – without data assimilation).

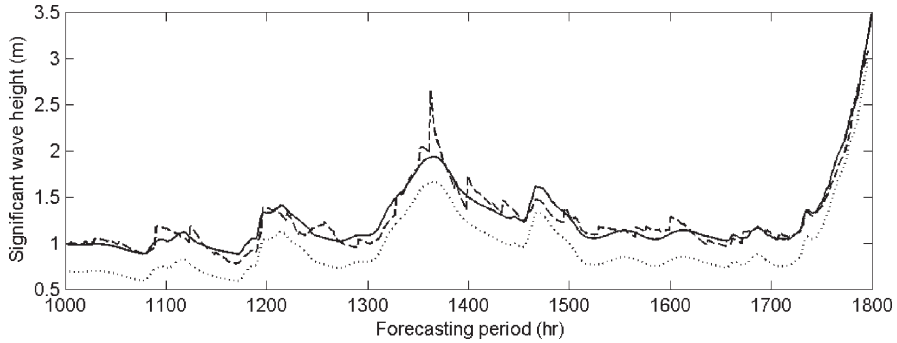

Figure 10 | Verification of ANN at point A (dashed line – with data assimilation, solid line – ANN training results, dotted line – without data assimilation).

One additional point is that rapid change in SWH with time is observed for the case with data assimilation, while a smoother change in the SWH with time is observed for the case using ANN. The reason is the distance between the output point and the position of the satellite changes rapidly at a certain period of time, which causes a rapid change in the functional value of P_{ik} in Equation (5). The input to the ANN is the computed waves without data assimilation, which is a smoother function with time. Thus the output from the ANN will also be a smooth continuous function.

CONCLUSIONS

Altimeter SWH data have been assimilated into a third-generation wave model by the statistical interpolation method to improve the accuracy of the model hindcasting

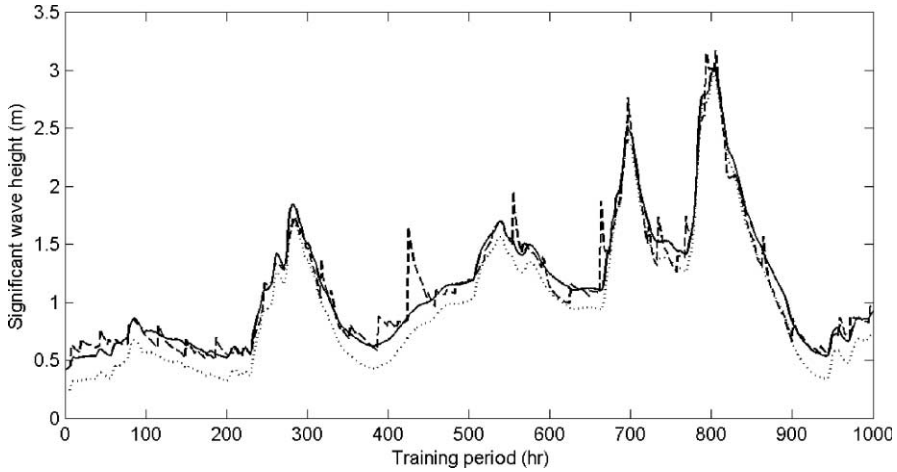

Figure 11 | Training of ANN at point B (dashed line – with data assimilation, solid line – ANN training results, dotted line – without data assimilation).

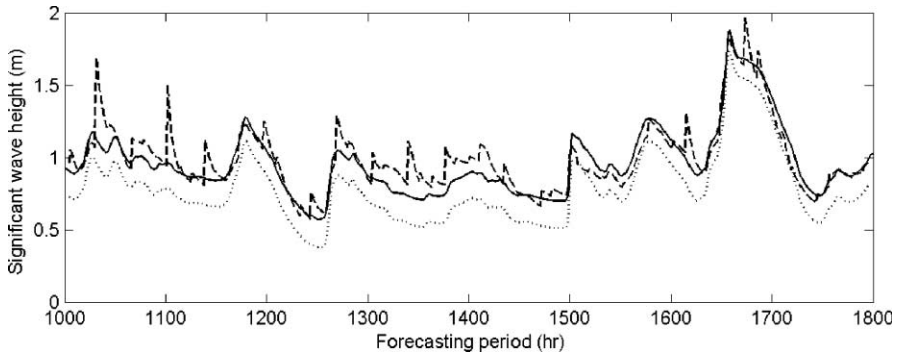

Figure 12 | Verification of ANN at point B (dashed line – with data assimilation, solid line – ANN training results, dotted line – without data assimilation).

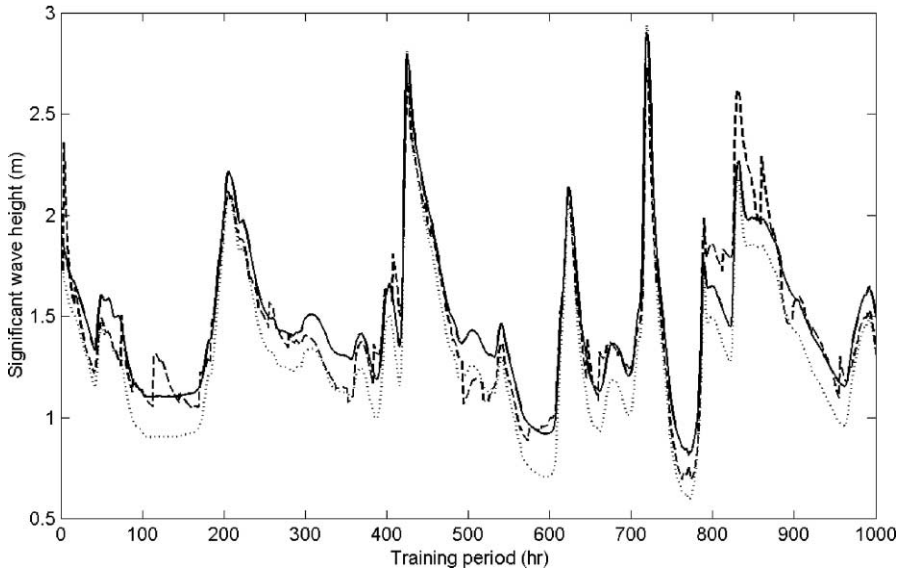

Figure 13 | Training of ANN at point C (dashed line – with data assimilation, solid line – ANN training results, dotted line – without data assimilation).

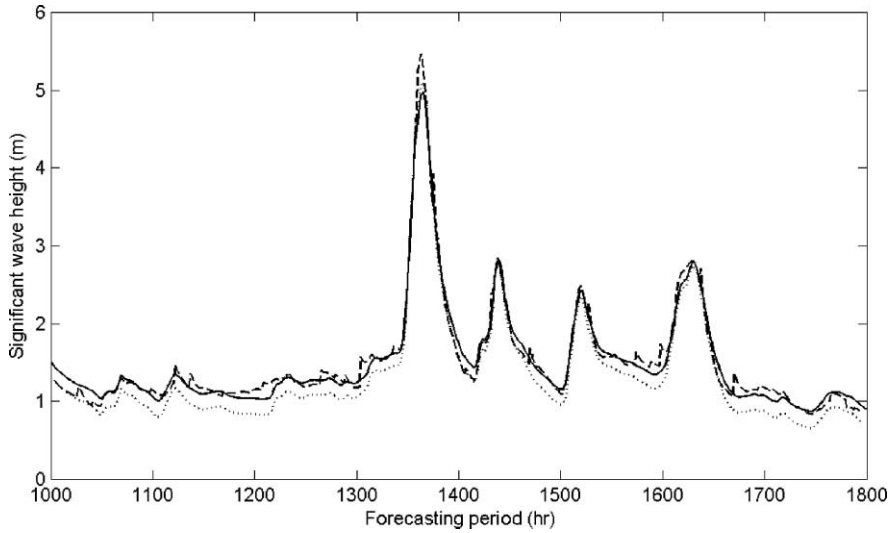

Figure 14 | Verification of ANN at point C (dashed line – with data assimilation, solid line – ANN training results, dotted line – without data assimilation).

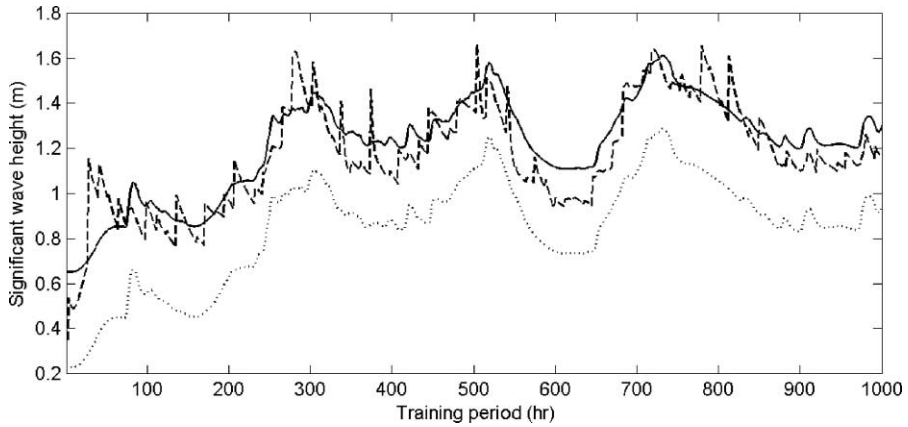

Figure 15 | Training of ANN at point D (dashed line – with data assimilation, solid line – ANN training results, dotted line – without data assimilation).

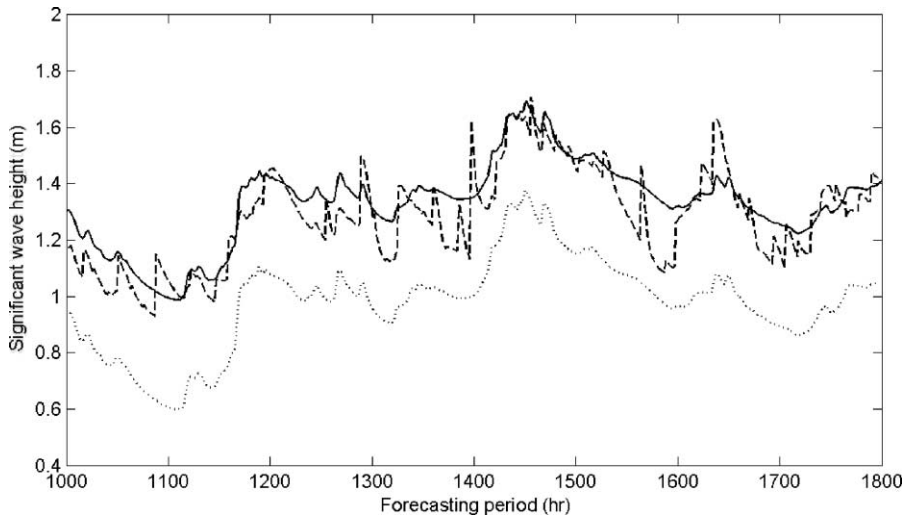

Figure 16 | Verification of ANN at point D (dashed line – with data assimilation, solid line – ANN training results, dotted line – without data assimilation).

of SWH. ANN has been introduced to mimic the effect of data assimilation and applied to situations where altimeter wave data are not available. By applying this approach to wind–wave simulation in the South China Sea, the results show that an apparent improvement in the accuracy of the forecasting can be obtained.

The training of ANN has been done for data in the summer period since typhoons in Hong Kong always occur during summer. This period is of most interest since extreme waves occur during typhoons. Seasonal variation in the wind system is significant and training of another ANN for other seasons will be required if waves in the other seasons are of interest.

ACKNOWLEDGEMENTS

This work was supported by a grant from the Research Grant Council of the Hong Kong Special Administrative Region (project no. PolyU 5051/00E) and a grant from the Hong Kong Polytechnic University (project no. A-PB74).

REFERENCES

Bauer, E., Hasselmann, S. & Hasselmann, K. 1992 Validation and assimilation of Seasat altimeter wave heights using the WAM wave model. *J. Geophys. Res.* **97**, 12671–12682.

Bauer, E., Hasselmann, K., Young, I. R. & Hasselmann, S. 1996 Assimilation of wave data into the wave model WAM using an impulse response function method. *J. Geophys. Res.* **101**, 3801–3816.

Bender, L. C. & Glowacki, T. 1996 The assimilation of altimeter data into the Australian wave model. *Aust. Meteorol. Mag.* **45**, 41–48.

Booij, N., Ris, R. C. & Holthuijsen, L. H. 1999 A third-generation wave model for coastal regions: 1. Model description and validation. *J. Geophys. Res.* **104** (C4), 7649–7666.

Deo, M. C. & Kumar, N. K. 2000 Interpolation of wave heights. *Ocean Engng.* **27**, 907–919.

Esteva, D. C. 1988 Evaluation of preliminary experiments assimilating Seasat significant wave heights into a spectral wave model. *J. Geophys. Res.* **93**, 14099–14106.

Francis, P. E. & Stratton, R. A. 1990 Some experiments to investigate the assimilation of Seasat altimeter wave height data in to a global wave model. *Q.J.R. Meteorol. Soc.* **116**, 1225–1251.

Gandin, L. S. 1963 *Objective analysis of meteorological fields*, Gidrometeoizdat, Leningrad (Translated from Russian by The Israeli Program for Scientific Translations, 1965).

Greenslade, D. J. M. 2001 The assimilation of ERS-2 significant wave height data in the Australian region. *J. Marine Syst.* **28**, 141–160.

Janssen, P. A. E. M., Komen, G. J. & de Voogt, W. J. P. 1984 An operational coupled hybrid wave prediction model. *J. Geophys. Res.* **89**, 3635–3654.

Komen, G. J. 1985 Introduction to wave models and assimilation of satellite data in wave models. In: *The Use of Satellite Data in Climate Models. Proc. Alpbach Conference. ESA Publ.* ESA SP 244, pp. 21–26.

Li, C. W. 1992 A split operator scheme for ocean wave simulation. *Int. J. Numer. Meth. Fluids* **15**, 579–593.

Li, C. W. 2000 Correlation of wave data sets at neighbour stations using artificial neural network with biased weighting of data. In: *Proc. 4th International Conference on Hydroinformatics* 262 (full paper on CD Rom), Balkema, Rotterdam.

Lionello, P., Günther, H. & Janssen, P. A. E. M. 1992 Assimilation of altimeter data in a global third-generation wave model. *J. Geophys. Res.* **97**, 14453–14474.

Refsgard, J. C. 1997 Validation and intercomparison of different updating procedures for real-time forecasting. *Nordic Hydrol.* **28**, 65–84.

Thomas, J. 1988 Retrieval of energy spectra from measured data for assimilation into a wave model. *Q. J. R. Meteoral. Soc.* **114**, 781–800.

Tolman, H. L. 1999 *User Manual and System Documentation of WAVEWATCH III version 1.18*. Tech. Note 166, NOAA/NWS/NECP/OMB.

Tsai, C.-P., Chang, L. & Shen, J.-N. 2002 Neural networks for wave forecasting among multi-stations. *Ocean Engng.* **29**, 1683–1695.

WAMDI Group (Hasselmann, S., Hasselmann, K., Bauer, E., Janssen, P. A. E. M., Komen, G. J., Bertotti, L., Lionello, P., Guillaume, A., Cardone, V. C., Greenwood, J. A., Reistad, M., Zambresky, L. & Ewing, J. A.) 1988 The WAM model - a third generation ocean wave prediction model. *J. Phys. Oceanogr.* **18**, 1775–1810.

Young, I. R. & Glowacki, T. J. 1996 Assimilation of altimeter wave height data into a spectral wave model using statistical interpolation. *Ocean Engng.* **23** (8), 667–689.